Toxicology in Vitro 83 (2022) 105415

Contents lists available at ScienceDirect

Toxicology in Vitro

journal homepage: www.elsevier.com/locate/toxinvit

Industrial-relevant TiO_2 types do not promote cytotoxicity in the A549 or TK6 cell lines regardless of cell specific interaction

Stephen J. Evans [a], Rachel L. Lawrence [a], Martha Ilett [b], Michael J. Burgum [a], Kirsty Meldrum [a], Nicole Hondow [b], Gareth J. Jenkins [a], Martin J.D. Clift [a], Shareen H. Doak [a,*]

[a] In Vitro Toxicology Group, Institute of Life Science, Swansea Univeristy Medical School, Swansea University, Singleton Park, Swansea, SA2 8PP, Wales, UK
[b] School of Chemical and Process Engineering, University of Leeds, Leeds LS2 9JT, UK

ARTICLE INFO

Editor: Dr. P Jennings

Keywords:
Titanium dioxide
Industrially relevant
Cytotoxicity
Cellular association
Cellular uptake

ABSTRACT

Due to the expansive application of TiO_2 and its variance in physico-chemical characteristics, the toxicological profile of TiO_2, in all its various forms, requires evaluation. This study aimed to assess the hazard of five TiO_2 particle-types in relation to their cytotoxic profile correlated to their cellular interaction, specifically in human lymphoblast (TK6) and type-II alveolar epithelial (A549) cells. Treatment with the test materials was undertaken at a concentration range of 1–100 μg/cm^2 over 24 and 72 h exposure. TiO_2 interaction with both cell types was visualised by transmission electron microscopy, supported by energy-dispersive X-ray. None of the TiO_2 materials tested promoted cytotoxicity in either cell type over the concentration and time range studied. All materials were observed to interact with the A549 cells and were further noted to be internalised following 24 h exposure. In contrast, only the pigmentary rutile was internalised by TK6 lymphoblasts after 24 h exposure. Where uptake was observed there was no evidence, as determined by 2D microscopy techniques, of particle localisation within the nucleus of either cell type. This study indicates that industrially relevant TiO_2 particles demonstrate cell interactions that are cell-type dependent and do not induce cytotoxicity at the applied dose range.

1. Introduction

Titanium dioxide (TiO_2) is a white inorganic compound with two main crystal structures: anatase and rutile, that both have diverse applications in industrial and consumer products (Yemmireddy and Hung, 2015). Industrially, TiO_2 is one of the most used pigments in paint due to its bright opaque colour, it is used in many food products as a colour and texture enhancer, as well as being widely used in cosmetic products as an ultraviolet (UV) absorber (Haider et al., 2019; Ropers et al., 2017; Fukui, 2018). Moreover, TiO_2 has been noted to have a number of potential environmental benefits *e.g.*, its use as paint on the outside of buildings in warm climates can reduce air-conditioning usage due to the materials' high refractive index (Li and Yang, 2019). Photocatalytic properties of TiO_2 under UV light can also be utilised to decompose environmental pollutants, for example, paint-comprised photopolymer resin and it is capable of efficiently degrading organic pollutants in water (Islam et al., 2020; Medvids et al., 2021). In the medical field TiO_2 has multiple pharmaceutical applications including as an inert tablet coating (Seo et al., 2020). Specific to the proposed industrial or consumer usage, TiO_2 is either used in bulk/pigment-grade (*i.e.* >100 nm) or nano form (*i.e.*, at least one dimension <100 nm) (Becker et al., 2014).

Due to the increased application of TiO_2 (and consequent, increased production) there is likely an increase in exposure risk, and thus the hazard potential of this material requires evaluation; both in the bulk and nano forms (Al-Mamun et al., 2019; Tetteh et al., 2021; Danfá et al., 2021). Annual world-wide pigmentary TiO_2 production capacity in metric tons rose from 5.7 million in 2010 to 8.4 million in 2020 and is predicted to rise further year on year (Bedinger, 2020). The physico-chemical characteristics of different TiO_2 materials can vary extensively in terms of size, surface chemistry, surface area, geometry, and crystal structure (Stefa et al., 2020). These variations are dependent on the source of the material *e.g.*, the atomic structure of rutile and anatase consist of an interconnected octahedra, however the degree of distortion of the octahedron differs between the two materials (Luttrell et al., 2014). This variation in crystallographic orientation of anatase and rutile also creates differences in surface reactivity properties, with anatase having a greater degree of free surface energy than rutile

* Corresponding author.
E-mail address: s.h.doak@swansea.ac.uk (S.H. Doak).

https://doi.org/10.1016/j.tiv.2022.105415
Received 9 December 2021; Received in revised form 7 March 2022; Accepted 4 June 2022
Available online 13 June 2022

(Selloni, 2008). Comparatively, TiO_2 nanoparticles have the potential to react at the cellular level in a different manner to bulk materials. This is due to the unique and potentially highly bio-reactive properties of materials at the nanoscale, such as increased surface area and consequently, increased surface reactivity (Oberdorster et al., 2005). An early TiO_2 study comparing the inflammatory effect of ultrafine (25 nm) and fine (250 nm) TiO_2 in the lungs of rats demonstrated no induction of inflammation caused by the fine material (Ferin et al., 1992). This contrasted with a chronic inflammatory response following exposure to the ultrafine material that lasted 14 days and subsequently subsided during the remaining fifty weeks of the study. A more recent study considered the impact of TiO_2 crystal structure on immune activity *in vitro* and *in vivo* using both immature dendritic cells (DCs) isolated from human peripheral blood monocytes and BALB/c mice (Vandebriel et al., 2018). The investigation highlighted that anatase forms promoted higher CD83 and CD86 expression *in vitro* over rutile forms. Moreover, instillation of anatase in mice lungs promoted neutrophil recruitment but rutile did not. A study by Danielsen et al. (2020) also came to this conclusion, in addition to attributing increased lung inflammation in the lungs of C57BL/6 J mice to increased TiO_2 surface area (Danielsen et al., 2020). Consequently various factors will influence the uptake potential of a (nano)particle including the physico-chemical properties of the material, cell type, variation in cell membrane characteristics, cell cycle time and exposure route (Adjei et al., 2014). A recent example has corelated increased cellular uptake of TiO_2 nanofibres with increased intercellular reactive oxygen species (ROS) production Particle-membrane interactions that facilitate internalisation by endocytic mechanisms would result in encapsulation of the material within an endosome where they may have the potential to escape into the cellular membrane, be transported intracellularly or through autophagy (Burgum et al., 2018). From a toxicological standpoint these factors can greatly influence the toxicity of any material including interference with organelle function and other cellular process or the production of cytoplasmic reactive oxygen species (ROS) by secondary cell types (Evans et al., 2019; Clift and Rothen-Rutishauser, 2013).

From an industrial, pharmaceutical, material science and regulatory standpoint, it is highly beneficial to gain an understanding of particle-cell interaction of materials such as TiO_2. Therefore, this current study aimed to assess the ability of five TiO_2 particle forms (a nano-sized anatase, two pigmentary rutile forms, a nano-sized rutile and pigmentary anatase; size range 10 nm to 1 μm) to be internalised and promote cytotoxicity in two different cell lines (lymphoblast (TK6) and type-II alveolar epithelial (A549) cells). The selection of these two cell types was based on the potential of the test materials to be inhaled in an industrial scenario (A549 cells) and to evaluate potential interactions with a well characterised cell type that is recommend for use in hazard characterisation (TK6 cell line) (OECD, 2014). Based on the available data in the literature, it was hypothesized that smaller anatase TiO_2 particles would have the potential for the greatest cellular interactions.

2. Materials and methods

All materials described below were purchased from Sigma-Aldrich UK, unless otherwise stated. All TiO_2 test materials were provided in powder form by the Titanium Dioxide Manufacturers Association (TDMA) and are listed in Table 1 (further physico-chemical data located in Supplementary Table 1).

Prior to cell culture exposures, the test materials G2–5, G3–1, G4–19 and E171-E were all sonicated as outlined in the NANOGENOTOX dispersion protocol in 6 ml 0.05% Bovine Serum Albumin in double distilled water (Jensen et al., 2016). Briefly, 15.36 mg (in glass scintillation vials) of each test material was pre-wetted with 30 μl of ethanol in a dropwise manner, 970 μl of 0.05% Bovine Serum Albumin (BSA) (Millipore, UK) solution was subsequently added while slowly rotating the vial at 45°. The suspension was then made up to a final volume of 6 ml by the addition of 5 ml 0.05% BSA solution. Test material G6–3 was prepared in the same manner but with the addition of 0.05% tween 80 to aid dispersion. Sonication of the sample suspensions was undertaken using a 400 W, 20 KHz Branson Sonifier S-450D (Branson Ultrasonics Corp, USA). In preparation for sonication the sample vials were placed into an ice water bath and the sonicator probe lowered one third into the material suspension. Sonication was undertaken for 16 min at an amplitude of 21%, on completion the dispersed samples remained stable for up to 60 min. Prior to cell treatments test materials were briefly vortexed (10 s).

All treatments with the test materials were performed in the units μg/cm^2 this was to ensure consistency between the exposure scenarios of both test cells lines (*i.e.*, submerged culture compared to an air-liquid interface). The doses were calculated as shown in Eq. (1), (test material surface areas are shown in Table 1).

Equation 1 – Calculating TiO_2 sample dose

$$\text{Surface Area Exposed (SAE)}\left(\text{cm}^2/\text{cm}^2\right) = \left[\text{Particles surface area}\left(\text{cm}^2\right) \times \text{Tissue culture surface area}\left(\text{cm}^2\right)\right] \times \text{Required dose}\left(\mu\text{g}/\text{cm}^2\right)$$

$$\text{Concentration of particles to achieve required dose}\left(\mu\text{g}/\text{ml}\right) = \left[\frac{\text{SAE}\left(\text{cm}^2/\text{cm}^2\right)}{\text{Volume of submerged exposure (ml)}}\right] \Big/ \text{Particle surface area}\left(\text{cm}^2\right)$$

2.1. Cell culture and treatment – TK6 cell line

The suspension B-lymphoblastoid cell line Thymine Kinase 6 (TK6) was purchased from the American Tissue Culture Collection (ATCC CRL-8015®). TK6 cells were cultured in Roswell Park Memorial Institute (RPMI)-1640 with 10% Horse serum (HS), 1% 200 mM L-glutamine and

Table 1
TiO_2 samples used in this study and their physico-chemical properties (data provided by TDMA) of G6–3 nanoscale particles, G2–5 nanoparticles, G3–1 pigmentary particles, G4–19 pigmentary particles, E171-E food grade pigmentary particles. Data is presented as the average +/− standard deviation (n = 3).

TiO_2	Average primary particle size (nm)[1]	Sizing by Disc Centrifuge in ddH_2O (nm)[2]	Surface area (BET) (m^2/g)[3]	Zeta potential (mV)[4]
G6–3 (rutile)	9.4 ± 2.3	342 ± 17.1	70 ± 3.5	−5.4 ± 0.27
G2–5 (anatase)	5.6 ± 1.2	301 ± 15.05	302 ± 15.1	−19.4 ± 0.97
G3–1 (rutile)	160.8 ± 71.3	379 ± 18.95	6 ± 0.3	−6.1 ± 0.31
G4–19 (rutile)	177.7 ± 58.4	191 ± 9.55	15 ± 0.75	−12 ± 0.6
E171-E (anatase)	106.8 ± 38.1	185 ± 9.25	10 ± 0.5	−54 ± 2.7

[1] Measured by scanning electron microscopy (SEM), [2]Measued by disc centrifugation sedimentation (DCS), [3] Measured by Brunauer-Emmett-Teller analyses (BET), [4]measured using a particle sizer (Horiba SZ-100).

1% streptomycin (100 μg/ml)/ penicillin (100 μg/ml) at 37 °C with 5% CO_2. Prior to sample treatment 2 ml 1×10^5 TK6 cells/ml were seeded in to 12-well plates and cultured for 24 hours (passage 5–10). For each TiO_2 sample, seven wells were seeded and treatments of 0, 1, 5, 10, 25, 50 and 100 μg/cm^2 were applied of the dispersed material (for each material type). All treatments were pre-diluted to the required concentration in complete culture media and 200 μl was added to each well. All treatments were performed in triplicate on three separate independent occasions for either 24 or 72 hours (n = 3).

2.2. Cell culture and treatment – A549 cell line

Adherent A549 lung epithelial type-II 'like' cells (ATCC CRL-185®) were cultured in RPMI-1640 with 10% Foetal Bovine Calf Serum (FBS), 1% 200 mM L-glutamine and 1% streptomycin (100 μg/ml)/ penicillin (100 μg/ml) at 37 °C with 5% CO_2. Before treatment, 2 ml 5×10^5 A549 cells/ml were seeded into the apical chambers of 4.2 cm^2 transwell inserts (6-well) and 3 ml of fresh complete media was added to the basal chamber. Cells were then cultured for 4 days at 37 °C, 5% CO_2. On the fourth day, the media was removed from the upper chamber and the lower chamber media replaced (3 ml) to enable the establishment of an air-liquid interface (ALI) (Barosova et al., 2021). For each TiO_2 sample, seven wells were seeded and treatments of 0, 1, 5, 10, 25, 50 and 100 μg/cm^2 applied of the pre-dispersed material using the quasi-ALI exposure method (Endes et al., 2014). All treatments were pre-diluted in complete culture media and 100 μl was added to each transwell insert.

2.3. Cytotoxicity assessment

2.3.1. Relative population doubling (RPD) and trypan blue assay for cytotoxicity assessment

Relative population doubling (RPD) analysis was used for assessing cell viability of TK6 cells following 24- and 72-h treatment with the test materials at 1, 5, 10, 25, 50 and 100 μg/cm^2 alongside an untreated and positive control 1 μg/ml mitomycin C (MMC)). An initial cell count was undertaken with a Coulter counter (Beckman, UK) prior to treatment which was used as the initial cell count number in Eq. (2) Treatment was then undertaken, and a post treatment cell count undertaken following the respective exposure period.

Equation 2 – RPD calculation

$$\text{RPD}\% = \frac{\text{Number of population doubling in treated cultures}}{\text{Number of population doubling in control cultures}} \times 100$$

Where population doubling = ***[***$\log$ ***(post treatment cell number/ initial cell number)]*** $\log$***2***

The trypan blue exclusion assay was used as a confirmatory cell viability assay in A549 cells treated with the highest dose of the test materials (100 μg/cm^2). Following treatment A549 cells were harvested, 100 μl of cell suspension was added to 100 μl of 0.4% trypan blue solution, loaded into a haemocytometer and the total number of cells and the number of non-viable cells counted under a 10× microscope objective (Zeiss Axio Vert, Carl Zeiss Ltd., UK). Cell viability was calculated as in Eq. (3).

Equation 3 – Percentage cell viability (trypan blue assay)

$$\%\text{Viable cells} = 1.00 - \frac{\text{Number of blue cells}}{\text{Number of total cells}} \text{ x } 100.$$

2.3.2. Propidium iodide (PI) staining and flow cytometry analysis of TK6 and A549 cells

PI analysis was used to assess cellular necrosis of TK6 and A549 cells following 24- and 72-h treatment with the test materials. This was applied as a confirmatory cytotoxicity assay at the highest applied dose (100 μg/cm^2) in the TK6 cell line following RPD analysis and across the full dose range (1–100 μg/cm^2) in the A549 cell line (cell treatments were undertaken as described in Section 2.1). Heat shock positive controls were utilised for both cell lines and prepared by heating 1×10^6 cells in PBS to 80 °C in a heat block for 3 mins (Janus et al., 2020). Following treatment, TK6 cells were pelleted at 230 g for 5 mins, washed 3 times by resuspension of the cell pellets in 5 ml room temperature PBS and re-centrifugation at 230 x*g* for 5 mins. A549 cells were washed 3 times in 2 ml room temperature PBS (both apical and basal chambers), prior to the addition of 1 ml 0.25% trypsin EDTA in the apical side of the transwells, 2 ml in the basal chamber and incubation at 37 °C w/5% CO_2 for 5 min. Following incubation, 3 ml of complete culture medium was added to the detached cells which were subsequently transferred to a 15 ml centrifuge tube, spun at 230 *g* for 5 mins and washed once in PBS.

Following harvesting, both cell lines were prepared in an identical manner; 1×10^6 cells were suspended in 1 ml room temperature PBS with 3 μM PI stain (Cat No. 421301, Biolegend, UK) and subsequently incubated in the dark at 4 °C for 1 h. Flow cytometry was undertaken using a NovoCyte Quanteon Flow Cytometer (Agilent, USA). Cells were excited by a 488 nm laser and red fluorescence (>600 nm) measured. Live/dead cell discrimination was based on the positive control (heat shock) for 10,000 events per sample. All samples were performed in triplicate on three separate independent occasions ($n = 3$). An example of the gating strategy is shown in Supplementary Fig. 1.

2.4. Cellular uptake assessment of test materials by TEM

Both TK6 and A549 cells were exposed with each test material at a concentration of 10 μg/cm^2. Subsequently 1×10^6 cells of each exposed cell population were fixed, embedded and sectioned. Sectioning and imaging was undertaken as previously described (Wills et al., 2016). Samples were examined using a FEI Titan3 Themis G2 S/TEM operated at 300 kV with an FEI Super-X energy dispersive X-ray (EDX) system and a Gatan OneView CCD camera. A total of 25 cells were imaged per cell type and test material at a magnification of x64,000 by high-angle annular dark field scanning TEM (HAADF-STEM). Where the presence of the test material was suspected within the tissue sections, elemental analysis was undertaken using EDX to provide confirmation of the elemental composition of the test material.

2.5. Assessment of nanoparticle association by flow cytometry

Side-scatter (SSC) and forward-scatter (FSC) data for each treatment was evaluated as described by Zucker et al. (2010). This allowed for assessment of potential interaction of the test materials with both cell types; based on the principle that increased light scatter due to reflection of the TiO_2 causes a greater side scatter and decreased forward scatter (Zucker et al., 2010). Thus, there is a shift in the cellular cache as seen through the flow cytometer. This enables the assessment as to whether the material is interacting with the cell system, or not, in a semi-quantifiable manner (example gating strategy shown in Supplementary Fig. 2). For each test material a percentage estimation of cellular interaction was made by comparing the SSC in treated cells to untreated cells (*i.e.*, negative control).

2.6. Data and statistical analysis

All data are presented as the mean +/− the standard deviation (SD). All analysis was completed over three independent biological replicates (n = 3). Statistical analysis was performed by the application of a One Way AVOVA with a Dunnett's *post hoc* test to determine if there was significance between control and treated values for all cytotoxicity assays used. A Pearson correlation coefficient calculation was performed to assess any corelation between the PI cytotoxicity and cell association data. All statistics were conducted using GraphPad PRISM software version 8 (GraphPad PRISM 8.4.3, USA) and considered significant if $p < 0.05$.

3. Results

This investigation aimed to assess the ability of five TiO_2 types to promote cytotoxicity in two different cell types (A549 and TK6) in relation to their cellular interactions. Cytotoxicity evaluation was initially undertaken by RPD analysis in the TK6 and A549 cell lines respectively. Confirmatory cytotoxicity analysis was undertaken by PI staining in TK6 cells and trypan blue counts in A549 cells. Selection of these assays was based on their suitability for each of the test cell lines with RPD analysis providing a measure of cytostasis/proliferation, trypan blue a measure of cell viability and PI staining a measure of cell death. Assessment of cellular interactions was undertaken by TEM and further analysis of the flow cytometry data. TEM analysis allowed for visual confirmation of TiO_2 uptake on a cell-by-cell basis and analysis of the flow cytometry data allowed for an estimation of cellular interaction (either cell surface interaction or cellular internalisation).

3.1. Assessment of TiO_2 cytotoxicity in TK6 cells

Viability assessment initially undertaken by RPD analysis following treatment of TK6 cells with test TiO_2 materials; G2–5, G4–19, G3–1, E171-E and G6–3 did not demonstrate any statistically significant ($p > 0.05$) decrease in cell survival at any of the applied concentrations (1–100 μg/cm^2) compared to the untreated controls (Fig. 1 a – j). This was consistent when the cells were treated for both 24- and 72- h. Cell survival was noted to be >95% following treatment will all concentrations of each test TiO_2 at each of these time points. Confirmatory analysis undertaken by PI staining indicated that approximately 80% of the cell population treated with the highest dose (100 μg/cm^2) of each test material was viable. This was consistent with the viability of the untreated control cells in all experiments. No statistically significant ($p > 0.05$) decrease in cell survival was noted following treatment with any of the test TiO_2 types when compared to the untreated control (Fig. 1 k – l).

3.2. Assessment of TiO_2 interaction with TK6 cells

Following cytotoxicity assessment approximately 25× TK6 cell sections (per material) were imaged by TEM following treatment with TiO_2 G2–5, G4–19, G3–1, E171-E and G6–3. Only G3–1; a rutile with a particle size of ~160 nm was observed to be internalised in this cell type (Fig.2 a). The internalised material was visible as an agglomerate of faceted electron dense particles localised in the cytoplasm of the cells consistent with their expected size, the observed material was confirmed as TiO_2 by EDX (representative image analysis shown in Fig. 3). No nuclear uptake was observed and there was no evidence of the material being associated with the cell surface when imaged by TEM. Flow cytometry analysis of 1000 cells was utilised to estimate association of the test materials with TK6 (Table 2). Evidence of association with 4.25%, 37.2%, 18%, and 30.8% with materials G3–1, G4–19, G6–3 and E171-E was observed with the TK6 cells. This estimation of interaction is an indication of the proportion of TK6 cells that have the test material associating either at the cell surface or following internalisation. This consequently implied test materials G4–19, G6–3, E171-E readily associated with the cell surface of TK6 cells (24 h exposure). There was no evidence of association between G2–5 (5.6 nm anatase) and the TK6 cell line. No correlation was observed between the cytotoxic and cellular association data of any of the test materials ($r = 0047$). Considering the physico-chemical characteristics of each test material, E171 -E and G4–19 both demonstrated the highest degree of cellular association with TK6 cells. Interestingly, both materials were shown to form the smallest agglomerates of the materials tested when measured by disc centrifugation, 185 (E171-E) and 191 nm (G4–19). The only material where cellular internalisation was observed by TEM, G2–5, did not conform to this trend as disc centrifuge measurements placed its size in suspension as 301 nm.

3.3. Assessment of TiO_2 cytotoxicity with A549 cells

Cytotoxicity assessment of A549 cells treated with test TiO_2 materials; G2–5, G4–19, G3–1, E171-E and G6–19 was firstly performed by PI flow cytometric analysis at an applied concentration range of 1–100 μg/cm^2. This analysis undertaken following both 24- and 72 h treatments indicated no significant ($p > 0.05$) decrease in cell survival in A549 cells treated with any of the test materials (Fig. 4 a - j). Following all treatments, the number of viable cells was always proportional to the number of viable cells in the untreated control populations and approximately >75% in all instances. Moreover, further cytotoxicity evaluation undertaken at the highest applied dose (100 μg/cm^2) by trypan blue staining also did not demonstrate any statistically significant ($p > 0.05$) decrease in cell survival (Fig. 2 k – l).

3.4. Assessment of TiO_2 interaction with A549 cells

Following cytotoxicity assessment, A549 cells were imaged in an identical manner to the TK6 cell line after treatment with the test materials. There was visual evidence of internalisation of all test TiO_2 materials in this cell type (Fig. 2 b – f). TiO_2 G3–1 (160 nm rutile) was typically visible in small agglomerates of 2–3 particles in vesicles in the cytoplasm. Similarly, small agglomerates of materials G2–5 (5.6 nm anatase) and G4–19 (177.7 nm rutile) were also localised in the vesicles. Materials E171–1 (106.6 nm anatase) and G6–3 (9.4 nm rutile) were localised in the cytoplasm but in seemingly larger agglomerates than the other TiO_2 types. The morphology of internalised G6–3 appeared more rod shaped compared to the faceted particle structure of the other test materials. Where uptake was suspected EDX analysis was undertaken to confirm the elemental composition of the observed material to be TiO_2 (representative image analysis shown in Fig. 3). Cellular association assessment by flow cytometry indicated interaction with 4.5%, 4.42%, 38%, 0.7% and 0.5% of the A549 cell population treated with materials G3–1, G4–19, G6–3 and E171-E respectively. No correlation was noted between the observed cellular interaction and cytotoxic potential of the test materials ($r = 0.0048$). Similarly, there appeared to be no corelation between cellular association of the test materials and their physico-chemical characteristics.

4. Discussion

TiO_2 particles in both its bulk and nanoscale form has become a material of great interest in recent years due to use in a wide range of consumer and industrial products (Dréno et al., 2019; Çeşmeli and Biray Avci, 2019; Elia et al., 2018). This investigation assessed the potential cytotoxicity (measured by RPD/PI stain analysis in TK6 cells and PI / trypan blue stain analysis in A549 cells) of industrially relevant TiO_2 samples; G6–3 (~9.4 nm), G2–5 (~ 14.2 nm), G3–1 (~160.8 nm), G4–19 (~177.7 nm) and E171-E (~106.8 nm) relative to their interaction with both TK6 (human B-lymphoblasts) and A549 (human lung type-II like epithelial) cells. This was determined by flow cytometry, and further their internalisation *via* TEM imaging. During this study it was noted that none of the test materials promoted cytotoxicity in either cell type at the applied dose range of 1–100 μg/cm^2. In the TK6 cell line only entry of material G3–1 was observed, however there was evidence of association of all test materials with this cell type when assessed by flow cytometry, denoting that the materials may be interacting at the cell surface with this suspension cell type (Zucker et al., 2010). In the A549 cell line, all materials demonstrated the potential to undergo cellular internalisation when visualised by TEM and assessed by flow cytometry analysis, demonstrating the potential for cellular association of all materials. A key difference between the two cell types being that TK6 is a suspension cell line and A549 is adherent likely played a role in the observed differences in cellular uptake. The test material may have had an increase potential of settling on the A549 cells, increasing the likelihood of cellular internalisation. Furthermore, A549 cells are an innate

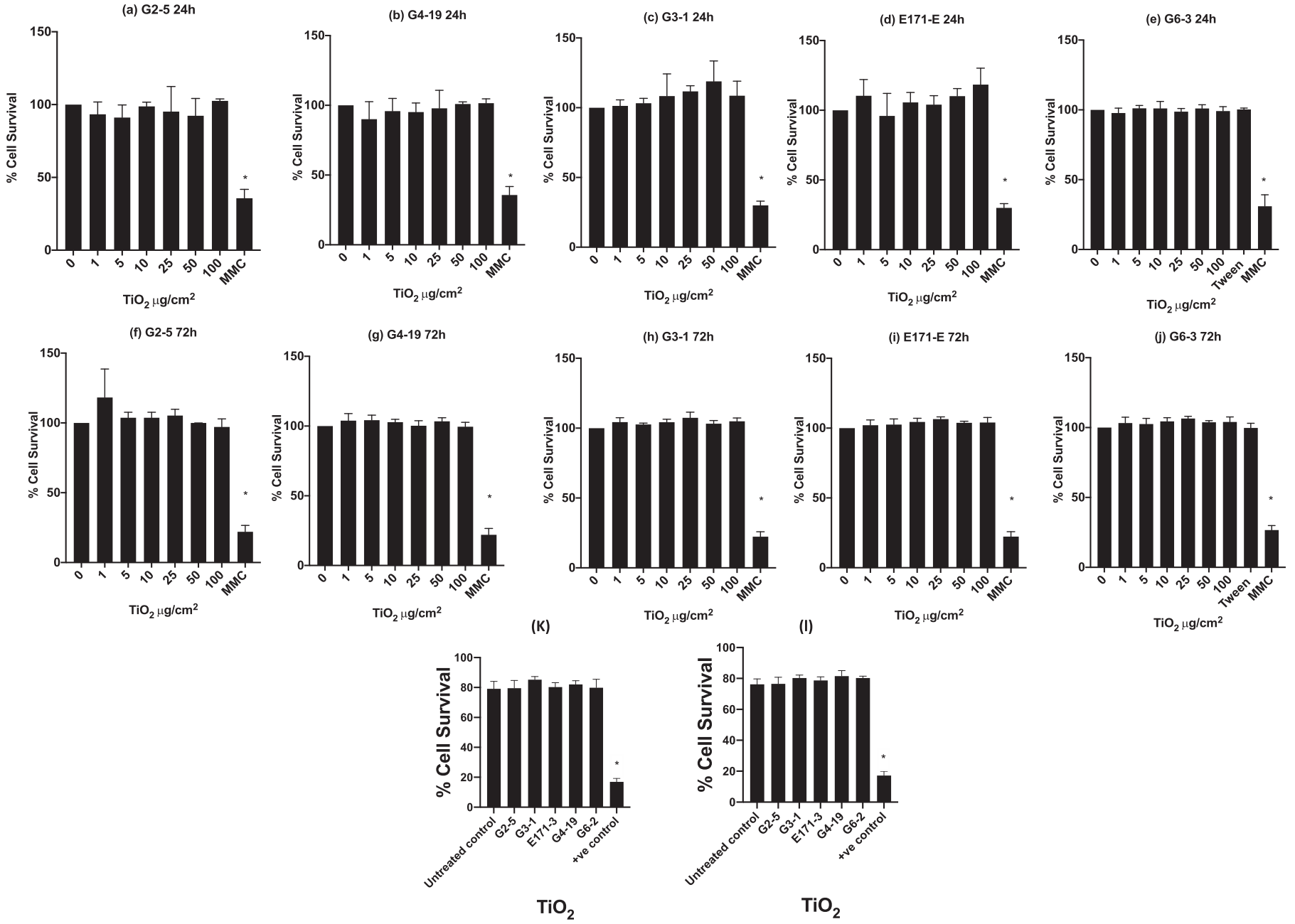

Fig. 1. Cytotoxicity assessment of TK6 cells treated with test materials. RPD analysis of TK6 cells treated with sample G2–5 (a), G4–19 (b), G3–1 (c), E171-E (d), G6–3 (e) for 24 h and G2–5 (f), G4–19 (g), G3–1 (h), E171-E (i) G6.3 (j) for 72 h. PI staining analysis of TK6 cell treated with all test materials for 24 h (k) and 72 (h). Both assays are presented demonstrating percentage cell survival of treated cells compared to untreated control. MMC (1 μg/ml) was used as a positive control for RPD assay and heat shock treatments used for PI analysis. *$p < 0.05$ when compared to untreated control ($n = 3$).

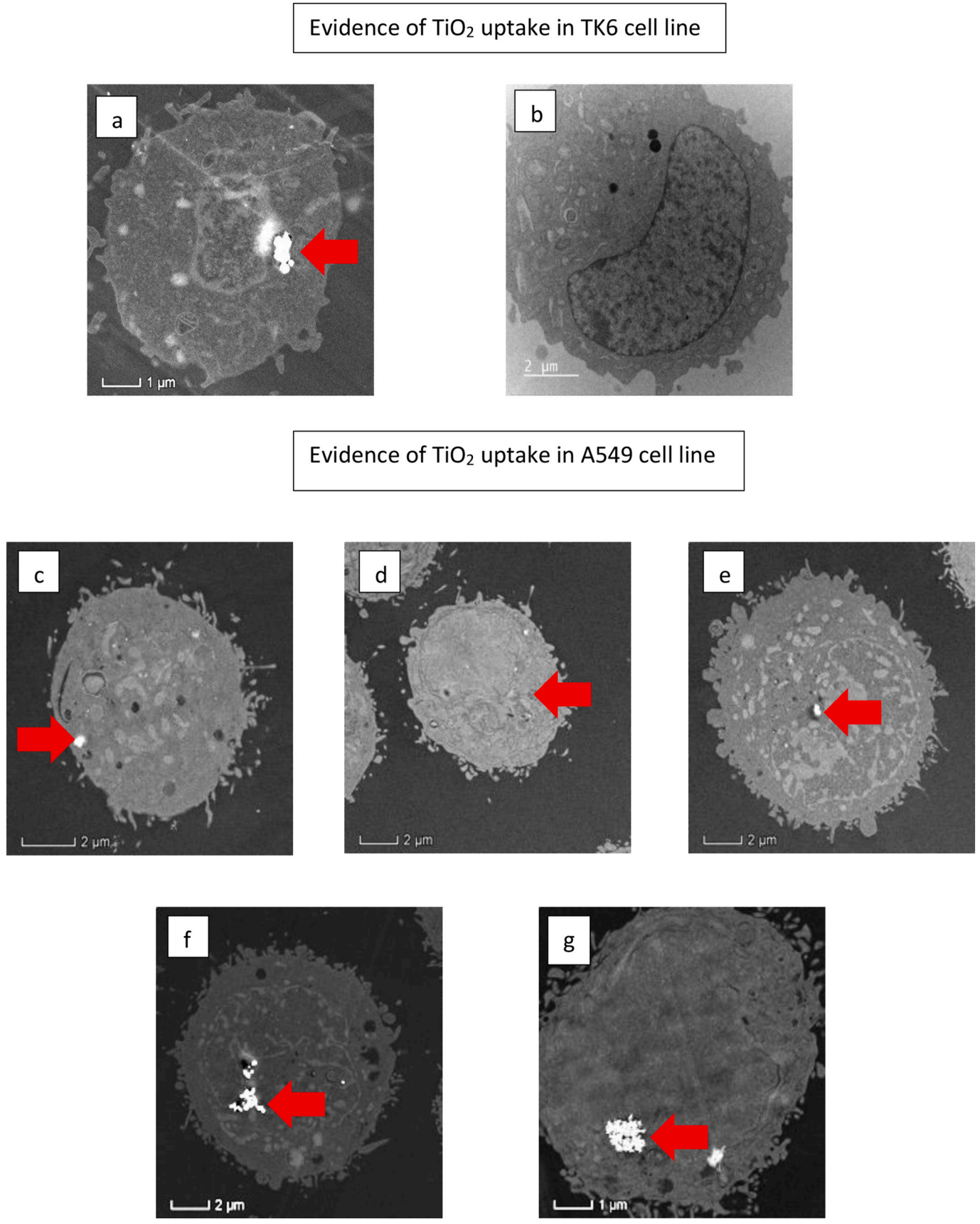

Fig. 2. TEM cellular uptake assessment of test materials – (a) G3–1 localised in cytoplasm of TK6 cell (b) Example TK6 cell with no evidence of material uptake as seen following exposure with G2–5, E171-E, G4–19 and G6–3. Whole A549 cell image with evidence of internalised material within the cytoplasm of G3–1 (c), G2–5 (d), E171-E (e), G4–19 (f) and G6–2 (g).

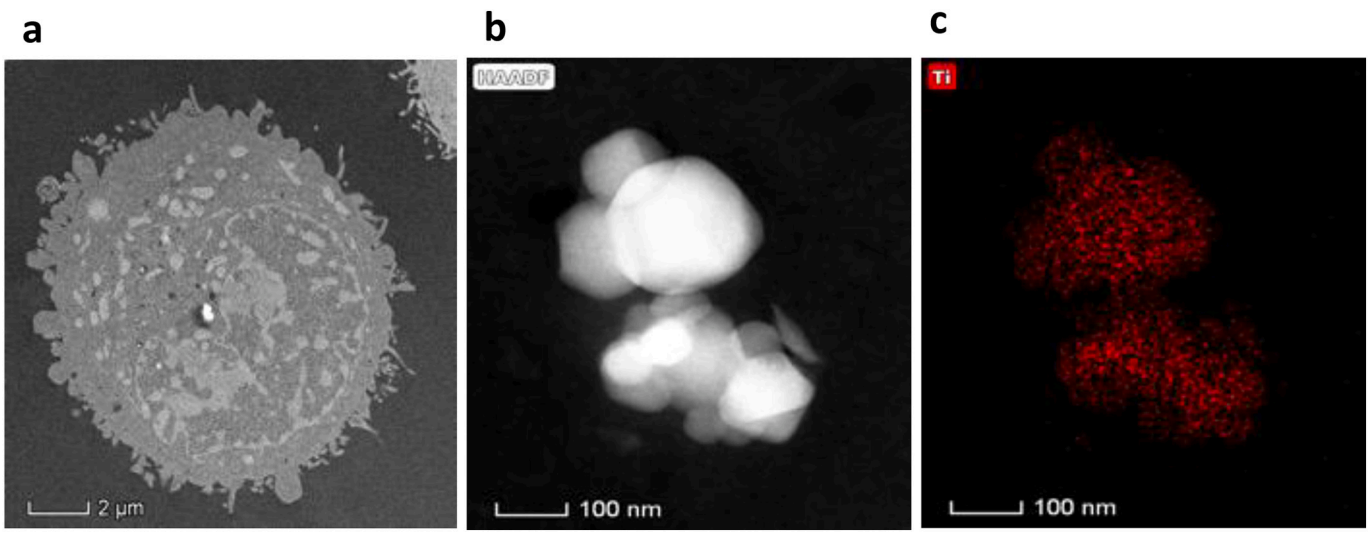

Fig. 3. Example of EDX elemental analysis used to confirm the presence of titanium (Ti) in suspected regions of test material uptake. (a) – STEM whole cell image with red arrow pinpointing internalised TiO_2 particles (b) High magnification of particles (c) EDX mapping identifying the presence of Ti particle region. (For interpretation of the references to colour in this figure legend, the reader is referred to the web version of this article.)

Table 2
Flow cytometry estimation of percentage cellular association of samples G3–1, G4–19, G6–19, E171-E and G2–5 with TK6 and A549 cells. Cellular association percentages were estimated using the gating strategy shown in Supplementary Fig. 2.

Sample	Evidence of cellular association – TK6 cells	Evidence of cellular association – A549 cells
G3–1	4.25% ± 0.22	4.5% ± 0.20
G4–19	37.2% ± 1.86	4.42% ± 0.19
G6–3	18% ± 0.9	38% ± 2.0
E171-E	30.8% ± 1.6	0.7% ± 0.1
G2–5	0% ± 0	0.5% ± 0.12

immune cell type, and it is likely that the test materials underwent uptake by endocytic mechanisms. Uptake inhibition studies have previously shown both caveolin- and clathrin- mediated uptake to be the key mechanisms of particle uptake in A549 cells (Kuhn et al., 2014).

The ability of any bulk or nano material to cause cell death or any adverse toxicological effect can be associated to its physico-chemical properties (Gatoo et al., 2014). Various studies have undertaken cytotoxicity evaluation of TiO_2 particles that have noted little to no induction of cytotoxicity. For example ~21 nm anatase nanoparticles were shown only to promote limited cytotoxicity (<30%) in A549 cells following a 48 h exposure period (Biola-Clier et al., 2016). Moreover, an investigation into the cytotoxic effect of TiO_2 nanofibers (101–400 nm) and nanoparticles (1–100 nm) in the A549 cell line cultured in both submerged and ALI conditions noted the fibres to have a significantly greater cytotoxic potential than nanoparticles, under both culture conditions (Medina-Reyes et al., 2020). Considering a different cell line, a recent study based on the BEAS-2B cells by Gea et al. highlighted the cytotoxicity of TiO_2 rods (108 nm), bi-pyramids (50 nm) and food grade particles (150 nm) showed only a slight decrease in cell survival at the highest applied doses (20, 50 and 80 µg/ml) (assessed by LDH assay) (Gea et al., 2019). Opposing this there are also studies which indicate TiO_2 particles to have significant cytotoxic potential and that this can be highly dependent on material size and crystalline state. TiO_2 (12 nm anatase) nanoparticles synthesised in house by Freire et al. (2021) were demonstrated to be cytotoxic, although only at high doses (>50 µg/ml) (Freire et al., 2021). Xiong et al. performed a cytotoxic comparison of three different sized anatase TiO_2 nanoparticles (10, 20 and 100 nm) and highlighted that decreased sized promoted increased cytotoxicity in both BEAS-2B and THP-1 cells (Xiong et al., 2013). Conversely, an investigation into the impact of TiO_2 physico-chemical characteristics on cytotoxicity highlighted that larger TiO_2 anatase nanoparticles were more cytotoxic than the smaller ones tested (Kose et al., 2020). The conflicting data on TiO_2 toxicity throughout the literature highlights the extensive variation in the materials tested and pinpoints a need to ensure that materials undergoing assessment are relevant to exposure risk.

It is interesting that despite the lack of cytotoxicity induction by any of the test TiO_2 particles in this current study, they all demonstrated the potential to undergo at least some degree of cellular association. A summary of the cellular interaction assessed in this study is listed in Table 3 in descending order of observed cellular uptake and interaction potential. The only test material wherein uptake was observed in both TK6 and A549 cell was the G3–1 sample, a rutile form with a primary particle size of ~160.8. nm. The crystalline structure of this material is perhaps a contributing factor in its ability to be internalised by both cell types. A study by Allouni et al., 2012 considered the crystalline state on the uptake potential of TiO_2 particles in human fibroblasts (L929) (Allouni et al., 2012). The investigation noted that TiO_2 in anatase form was more likely to undergo cellular uptake than rutile TiO_2. Another *in vitro* study conducted with the Caco-2 cell line (human intestinal cells) also demonstrated that anatase underwent cellular uptake whereas rutile did not, the investigation suggested this was due to anatase being better detected at the cell surface allowing the initiation of clathrin-mediated endocytosis, although this was not elaborated on further (Gitrowski et al., 2014). It is probably that this increased likelihood of cellular association with anatase as opposed to rutile TiO_2 is due to differing surface energies caused by distorted tetragonal atomic arrangement (Selloni, 2008). G3–1 had the second largest primary particle size in this study, potentially indicating that size had an impact on uptake potential. A primary particle size of 160.8 ± 71.3 nm would place G3–1 in a suitable size range to undergo clathrin-mediated endocytosis as would the sizes of materials G4–19 and E171-E (~177.7 and ~ 106.8 nm respectively), both of which underwent uptake by the A549 cell line (Foroozandeh and Aziz, 2018). Despite the observed internalisation of G3–1 by both cell types, evidence of cellular interaction with this material appears to be limited when evaluated by flow cytometry. This limited interaction may be attributed to lower reactivity due to a larger surface area of this material compared to the smaller particle sizes of other materials tested. Sample E171-E (anatase) for instance was shown to interact with ~37.2% of the TK6 cell population compared to G3–1 where interaction was shown with only 4.25%

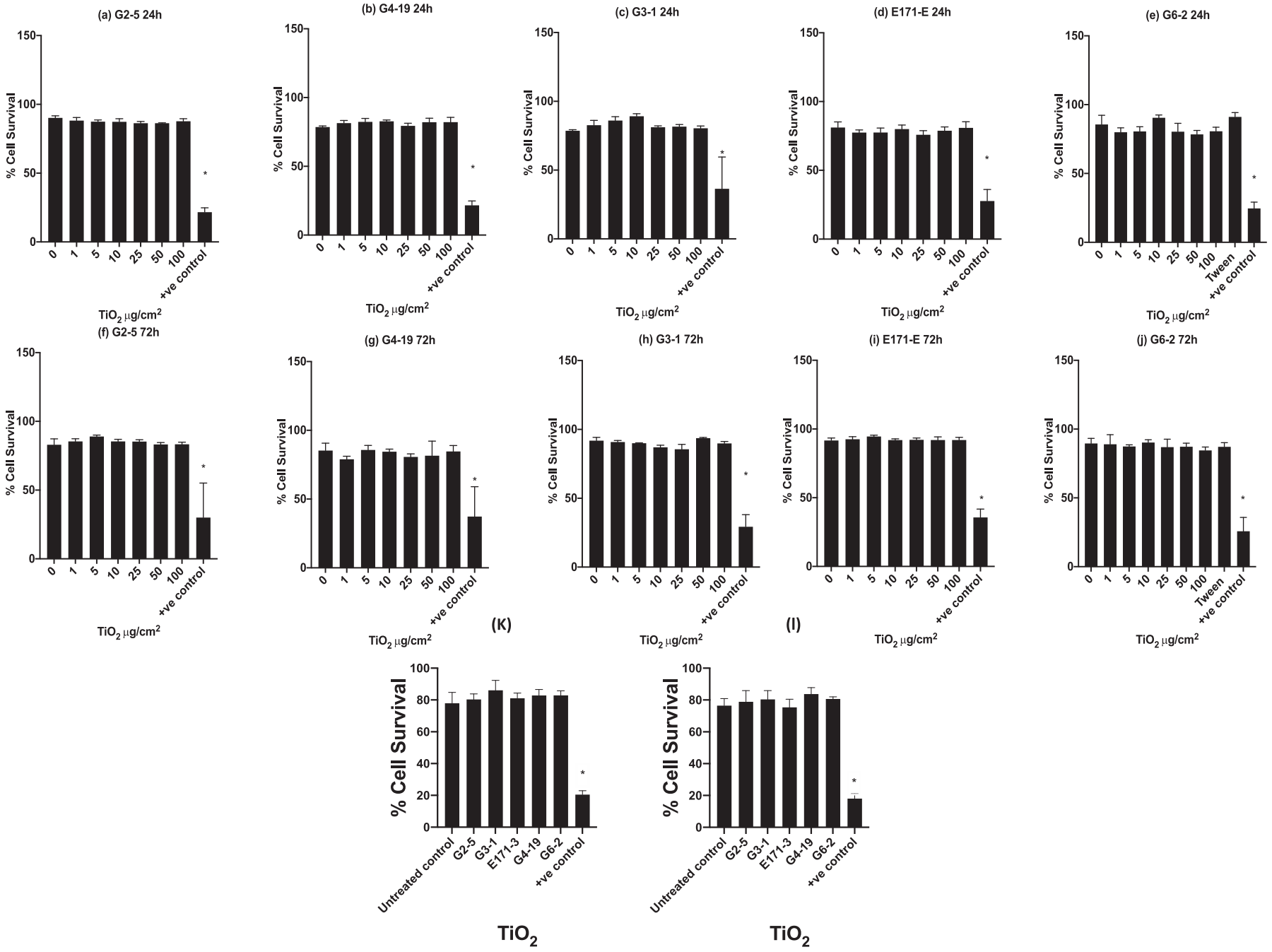

Fig. 4. Cytotoxicity assessment of A549 cells treated with test materials. PI staining analysis of A549 cells treated with sample G2–5 (a), G4–19 (b), G3–1 (c), E171-E (d), G6–3 (e) for 24 h and G2–5 (f), G4–19 (g), G3–1 (h), E171-E (i) G6.3 (j) for 72 h. Trypan blue staining analysis of A549 cells treated with all test materials for 24 h (k) and 72 (l). Both assays are presented demonstrating percentage of cell survival of treated cells compared to untreated control. MMC (1 μg/ml) was used as a positive control. *$p < 0.05$ when compared to untreated control ($n = 3$). (For interpretation of the references to colour in this figure legend, the reader is referred to the web version of this article.)

Table 3
Summary of cellular interaction (cytotoxicity, cellular uptake and cellular association) of test materials G3–1, G4–19, G6–19, E171-E and G2–5 with the TK6 and A549 cell lines. Estimation of percentage cellular association was undertaken as described in Section 3.6. Test materials are listed in descending order of observed cellular uptake and interaction potential (*) denotes an observed effect, (–) denotes no observed effect.

Sample	TK6 cell line			A549 cell line		
	Cytotoxicity	Evidence of cellular uptake	Evidence of cellular association	Cytotoxicity	Evidence of cellular uptake	Evidence of cellular association
G3–1 (rutile)	–	*	* (4.25%)	–	*	* (4.5%)
G4–19 (rutile)	–	–	* (37.2%)	–	*	* (4.42%)
G6–3 (rutile)	–	–	* (18%)	–	*	* (38%)
E171-E (anatase)	–	–	* (30.8%)	–	*	* (0.7%)
G2–5 (anatase)	–	–	–	–	*	* (0.5%)

of the population. The average particle size of E171-E was ~50 nm smaller than G3–1, thus E171-E has a greater surface to volume ratio and potentially higher bio-reactivity (Suttiponparnit et al., 2011). Despite the greater degree of cellular interaction by E171-E, no uptake of this material was observed in TK6 cells, suggesting that its smaller size (in comparison with G3–1) potentially prevented uptake. In contrast however, there was evidence of E171-E uptake in the A549 cell line but with limited cellular association. It is a primary toxicological concern that a material <100 nm in size may have greater potential to undergo cellular uptake compared to a bulk material (Oberdorster et al., 2005). However, the TiO_2 samples investigated here do not strictly conform to this, with an anatase that is ~5.6 nm (sample G2–5) in size showing the potentially lowest cellular uptake and interaction potential.

Regardless of the cellular uptake and association data generated in this current study there was no observed correlation between increased uptake/cell surface association and a cytotoxic repose as none of the test materials caused cell death at the applied dose range ($r = 0.0048$). This is consistent with a (genotoxicity) study that undertook cytotoxicity and cellular uptake evaluation in 4 different cell lines (A549, HEPG2, A172 and SH-SY5Y) (Brandão et al., 2020). This investigation described that, regardless of a time dependant increase in cellular uptake of (25 nm) anatase particles, there was no increase in cell cytotoxicity in any of the test cell types, nor any observed genotoxicity.

4.1. Conclusions

In conclusion, the data gathered in this study demonstrates that the industrially relevant TiO_2 cellular interaction was dependent on the cell type used. The only TiO_2 particle-types in this study that were internalised by the TK6 cells was a rutile form with a primary particle size >160 nm, whereas all the TiO_2 test materials were shown to be internalised by A549 cells. Comparing the crystalline structure of the materials tested, the rutile materials appeared to have a greater potential to undergo cellular association, which differs from the initial proposed hypothesis. Regardless of cellular interactions, none of the TiO_2 particles induced cytotoxicity.

Funding sources

This study was funded by the Titanium Dioxide Manufacturers Association (TDMA).

Author contributions

Stephen J. Evans: Conceptulization, Methodology, Formal analysis, Validaion, Writing - orginal draft. Rachel L. Lawrence: Methology, Formal analysis, Writing - review & editing. Martha Ilet: Methology, Formal analysis, Writing - review & editing. Michael J. Burgum: Methology, Formal analysis, Writing - review & editing. Kirsty Meldrum: Methology, Formal analysis, Writing - review & editing. Nicole Hondow: Conceptulization, Methology, Formal analysis, Writing - review & editing. Gareth J. Jenkins: Writing - review & editing. Martin J. D. Clift: Conceptulization, Formal Analysis, Supervision. Shareen H. Doak: Conceptulization, Formal Analysis, Supervision.

Declaration of Competing Interest

None.

Acknowledgements

The authors would like to thank EBRC consulting and Titanium Dioxide Manufacturers Association (TDMA) for the provision of the test materials and the scientific discussions. We would also like to thank our colleagues from IVTG at Swansea University and The School of Chemical and Process Engineering at Leeds University for their support.

Appendix A. Supplementary data

Supplementary data to this article can be found online at https://doi.org/10.1016/j.tiv.2022.105415.

References

Adjei, I.M., Sharma, B., Labhasetwar, V., 2014. Nanoparticles: cellular uptake and cytotoxicity. Adv. Exp. Med. Biol. 811, 73–91.
Allouni, Z.E., Høl, P.J., Cauqui, M.A., Gjerdet, N.R., Cimpan, M.R., 2012. Role of physicochemical characteristics in the uptake of TiO_2 nanoparticles by fibroblasts. Toxicol. in Vitro 26, 469–479.
Al-Mamun, M.R., Kader, S., Islam, M.S., Khan, M.Z.H., 2019. Photocatalytic activity improvement and application of UV-TiO_2 photocatalysis in textile wastewater treatment: a review. J. Environ. Chem. Eng. 7, 103248.
Barosova, H., Meldrum, K., Karakocak, B.B., Balog, S., Doak, S.H., Petri-fink, A., Clift, M. J.D., Rothen-rutishauser, B., 2021. Inter-laboratory variability of A549 epithelial cells grown under submerged and air-liquid interface conditions. Toxicol. in Vitro 75, 105178.
Becker, K., Schroecksnadel, S., Geisler, S., Carriere, M., Gostner, J.M., Schennach, H., Herlin, N., Fuchs, D., 2014. TiO_2 nanoparticles and bulk material stimulate human peripheral blood mononuclear cells. Food Chem. Toxicol. 65, 63–69.
Bedinger, G.M., 2020. Titanium and Titanium Dioxide [Online]. Available. https://pubs.usgs.gov/periodicals/mcs2021/mcs2021-titanium.pdf.
Biola-Clier, M., Beal, D., Caillat, S., Libert, S., Armand, L., Herlin-Boime, N., Sauvaigo, S., Douki, T., Carriere, M., 2016. Comparison of the DNA damage response in BEAS-2B and A549 cells exposed to titanium dioxide nanoparticles. Mutagenesis 32, 161–172.
Brandão, F., Fernández-Bertólez, N., Rosário, F., Bessa, M.J., Fraga, S., Pásaro, E., Teixeira, J.P., Laffon, B., Valdiglesias, V., Costa, C., 2020. Genotoxicity of $TiO_{(2)}$ nanoparticles in four different human cell lines (A549, HEPG2, A172 and SH-SY5Y). Nanomat. (Basel, Switzerland) 10, 412.
Burgum, M.J., Evans, S.J., Jenkins, G.J., Doak, S.H., Clift, M.J.D., 2018. Chapter 10 - considerations for the human health implications of Nanotheranostics. In: Conde, J. (Ed.), Handbook of Nanomaterials for Cancer Theranostics. Elsevier.
Çeşmeli, S., Biray Avci, C., 2019. Application of titanium dioxide (TiO2) nanoparticles in cancer therapies. J. Drug Target. 27, 762–766.
Clift, M.J.D., Rothen-Rutishauser, B., 2013. Studying the oxidative stress paradigm in vitro: A theoretical and practical perspective. In: Armstrong, D., Bharali, D.J. (Eds.), Oxidative Stress and Nanotechnology: Methods and Protocols. Humana Press, Totowa, NJ.
Danfá, S., Martins, R.C., Quina, M.J., Gomes, J., 2021. Supported TiO_2 in ceramic materials for the photocatalytic degradation of contaminants of emerging concern in liquid effluents: A review. Molecules 26, 5363.
Danielsen, P.H., Knudsen, K.B., Štrancar, J., Umek, P., Koklič, T., Garvas, M., Vanhala, E., Savukoski, S., Ding, Y., Madsen, A.M., Jacobsen, N.R., Weydahl, I.K., Berthing, T., Poulsen, S.S., Schmid, O., Wolff, H., Vogel, U., 2020. Effects of physicochemical

properties of TiO2 nanomaterials for pulmonary inflammation, acute phase response and alveolar proteinosis in intratracheally exposed mice. Toxicol. Appl. Pharmacol. 386, 114830.
Dréno, B., Alexis, A., Chuberre, B., Marinovich, M., 2019. Safety of titanium dioxide nanoparticles in cosmetics. J. Eur. Acad. Dermatol. Venereol. 33, 34–46.
Elia, H., Ghosh, A., Akhnoukh, A., Nima, Z., 2018. Using nano-and micro-titanium dioxide (TiO_2) in concrete to reduce air pollution. J. Nanomed. Nanotechnol. 9, 1000505.
Endes, C., Schmid, O., Kinnear, C., Mueller, S., Camarero-Espinosa, S., Vanhecke, D., Foster, E.J., Petri-Fink, A., Rothen-Rutishauser, B., Weder, C., Clift, M.J.D., 2014. An in vitro testing strategy towards mimicking the inhalation of high aspect ratio nanoparticles. Part. Fibre Toxicol. 11, 40.
Evans, S.J., Clift, M.J., Singh, N., Wills, J.W., Hondow, N., Wilkinson, T.S., Burgum, M.J., Brown, A.P., Jenkins, G.J., Doak, S.H., 2019. In vitro detection of secondary mechanisms of genotoxicity induced by engineered nanomaterials. Part. Fibre Toxicol. 16, 1–14.
Ferin, J., Oberdörster, G., Penney, D.P., 1992. Pulmonary retention of ultrafine and fine particles in rats. Am. J. Respir. Cell Mol. Biol. 6, 535–542.
Foroozandeh, P., Aziz, A.A., 2018. Insight into cellular uptake and intracellular trafficking of nanoparticles. Nanoscale Res. Lett. 13, 1–12.
Freire, K., Ordóñez Ramos, F., Soria, D.B., Pabón Gelves, E., Di Virgilio, A.L., 2021. Cytotoxicity and DNA damage evaluation of TiO_2 and ZnO nanoparticles. Uptake in lung cells in culture. Toxicol. Res. 10, 192–202.
Fukui, H., 2018. Application 1 - development of new cosmetics based on nanoparticles. In: Naito, M., Yokoyama, T., Hosokawa, K., Nogi, K. (Eds.), Nanoparticle Technology Handbook, (Third Edition). Elsevier.
Gatoo, M.A., Naseem, S., Arfat, M.Y., Mahmood Dar, A., Qasim, K., Zubair, S., 2014. Physicochemical properties of nanomaterials: implication in associated toxic manifestations. Biomed. Res. Int. 2014, 8.
Gea, M., Bonetta, S., Iannarelli, L., Giovannozzi, A.M., Maurino, V., Bonetta, S., Hodoroaba, V.-D., Armato, C., Rossi, A.M., Schilirò, T., 2019. Shape-engineered titanium dioxide nanoparticles (TiO_2-NPs): cytotoxicity and genotoxicity in bronchial epithelial cells. Food Chem. Toxicol. 127, 89–100.
Gitrowski, C., Al-Jubory, A.R., Handy, R.D., 2014. Uptake of different crystal structures of TiO_2 nanoparticles by Caco-2 intestinal cells. Toxicol. Lett. 226, 264–276.
Haider, A.J., Jameel, Z.N., Al-Hussaini, I.H.M., 2019. Review on: titanium dioxide applications. Energy Procedia 157, 17–29.
Islam, M.T., Dominguez, A., Turley, R.S., Kim, H., Sultana, K.A., Shuvo, M.A.I., Alvarado-Tenorio, B., Montes, M.O., Lin, Y., Gardea-Torresdey, J., Noveron, J.C., 2020. Development of photocatalytic paint based on TiO2 and photopolymer resin for the degradation of organic pollutants in water. Sci. Total Environ. 704, 135406.
Janus, P., Toma-Jonik, A., Vydra, N., Mrowiec, K., Korfanty, J., Chadalski, M., Widłak, P., Dudek, K., Paszek, A., Rusin, M., Polańska, J., Widłak, W., 2020. Pro-death signaling of cytoprotective heat shock factor 1: upregulation of NOXA leading to apoptosis in heat-sensitive cells. Cell Death & Differentiation 27, 2280–2292.
Jensen, K., Booth, A., Kembouche, Y., Boraschi, D., 2016. Validated protocols for test item preparation for key in vitro and Ecotoxicity studies. NANoREG Deliverable D2, 06.
Kose, O., Tomatis, M., Leclerc, L., Belblidia, N.-B., Hochepied, J.-F., Turci, F., Pourchez, J., Forest, V., 2020. Impact of the physicochemical features of TiO_2 nanoparticles on their in vitro toxicity. Chem. Res. Toxicol. 33, 2324–2337.
Kuhn, D.A., Vanhecke, D., Michen, B., Blank, F., Gehr, P., Petri-Fink, A., Rothen-Rutishauser, B., 2014. Different endocytotic uptake mechanisms for nanoparticles in epithelial cells and macrophages. Beilstein J. Nanotechnol. 5, 1625–1636.
Li, Y., Yang, Y., 2019. Study on Preparation and thermal reflective properties of energy saving pigments with selective solar reflection. In: IOP Conference Series: Materials Science and Engineering. IOP Publishing, p. 012010.
Luttrell, T., Halpegamage, S., Tao, J., Kramer, A., Sutter, E., Batzill, M., 2014. Why is anatase a better photocatalyst than rutile? - model studies on epitaxial TiO_2 films. Sci. Rep. 4, 4043.
Medina-Reyes, E.I., Delgado-Buenrostro, N.L., Leseman, D.L., Déciga-Alcaraz, A., He, R., Gremmer, E.R., Fokkens, P.H., Flores-Flores, J.O., Cassee, F.R., Chirino, Y.I., 2020. Differences in cytotoxicity of lung epithelial cells exposed to titanium dioxide nanofibers and nanoparticles: comparison of air-liquid interface and submerged cell cultures. Toxicol. in Vitro 65, 104798.
Medvids, A., Onufrijevs, P., Kaupužs, J., Eglitis, R., Padgurskas, J., Zunda, A., Mimura, H., Skadins, I., Varnagiris, S., 2021. Anatase or rutile TiO_2 nanolayer formation on Ti substrates by laser radiation: mechanical, photocatalytic and antibacterial properties. Opt. Laser Technol. 138, 106898.
Oberdorster, G., Oberdorster, E., Oberdorster, J., 2005. Nanotoxicology: an emerging discipline evolving from studies of ultrafine particles. Environ. Health Perspect. 113, 823–839.
OECD, 2014. Test No. 487: In Vitro Mammalian Cell Micronucleus Test. OECD Publishing.
Ropers, M.-H., Terrisse, H., Mercier-Bonin, M., Humbert, B., 2017. Titanium dioxide as food additive. In: Tech Rijeka.
Selloni, A., 2008. Anatase shows its reactive side. Nat. Mater. 7, 613–615.
Seo, K.-S., Bajracharya, R., Lee, S.H., Han, H.-K., 2020. Pharmaceutical application of tablet film coating. Pharmaceutics 12, 853.
Suttiponparnit, K., Jiang, J., Sahu, M., Suvachittanont, S., Charinpanitkul, T., Biswas, P., 2011. Role of surface area, primary particle size, and crystal phase on titanium dioxide nanoparticle dispersion properties. Nanoscale Res. Lett. 6, 1–8.
Tetteh, E.K., RathilaL, S., Asante-Sackey, D., Chollom, M.N., 2021. Prospects of synthesized magnetic TiO_2-based membranes for wastewater treatment: a review. Materials 14, 3524.
Vandebriel, R.J., Vermeulen, J.P., Van Engelen, L.B., De Jong, B., Verhagen, L.M., De La Fonteyne-Blankestijn, L.J., Hoonakker, M.E., De Jong, W.H., 2018. The crystal structure of titanium dioxide nanoparticles influences immune activity in vitro and in vivo. Part. Fibre Toxicol. 15, 9.
Wills, J.W., Hondow, N., Thomas, A.D., Chapman, K.E., Fish, D., Maffeis, T.G., Penny, M. W., Brown, R.A., Jenkins, G.J., Brown, A.P., White, P.A., Doak, S.H., 2016. Genetic toxicity assessment of engineered nanoparticles using a 3D in vitro skin model (EpiDerm). Part. Fibre Toxicol. 13, 016–0161.
Xiong, S., George, S., Ji, Z., Lin, S., Yu, H., Damoiseaux, R., France, B., Ng, K.W., Loo, S.C. J., 2013. Size of TiO(2) nanoparticles influences their phototoxicity: an in vitro investigation. Arch. Toxicol. 87, 99–109.
Yemmireddy, V.K., Hung, Y.-C., 2015. Selection of photocatalytic bactericidal titanium dioxide (TiO_2) nanoparticles for food safety applications. LWT Food Sci. Technol. 61, 1–6.
Zucker, R.M., Massaro, E.J., Sanders, K.M., Degn, L.L., Boyes, W.K., 2010. Detection of TiO_2 nanoparticles in cells by flow cytometry. Cytometry A 77, 677–685.